In Silico Evaluation of Anti-Inflammatory Flavonoids from Marrubium vulgare L.: DFT Reactivity, Molecular Docking with COX Isozymes, Molecular Dynamic Simulation and Toxicity Prediction

Fatima Kadri
University of Science and Technology of Oran Mohamed BOUDIAF (USTO-MB)
Sofiane Benmetir
sofiane.benmetir@univ-usto.dz

University of Science and Technology of Oran Mohamed BOUDIAF (USTO-MB)
Mohammed Arab Ait Tayeb
University of Science and Technology of Oran Mohamed BOUDIAF (USTO-MB)
Khadidja Smail
University of Science and Technology of Oran Mohamed BOUDIAF (USTO-MB)
Fatima Zohra Fadel
University of Science and Technology of Oran Mohamed BOUDIAF (USTO-MB)
Karim Ouadah
University of Science and Technology of Oran Mohamed BOUDIAF (USTO-MB)
Noureddine Tchouar
University of Science and Technology of Oran Mohamed BOUDIAF (USTO-MB)
Jesus Vicente Julián-Ortiz
University of Valencia

Research Article

Keywords: Marrubium vulgare L., Flavonoids, Anti-inflammatory activity, COX-1, COX-2, DFT, Molecular Docking, Molecular Dynamics

Posted Date: October 10th, 2025

DOI: https://doi.org/10.21203/rs.3.rs-7601276/v1

Additional Declarations: No competing interests reported.

Version of Record: A version of this preprint was published at Theoretical Chemistry Accounts on May 20th, 2026. See the published version at https://doi.org/10.1007/s00214-026-03300-1.

Abstract

Chronic inflammation is a major contributor to the pathophysiology of numerous diseases, including cardiovascular disorders, neurodegeneration, and cancer. Although non-steroidal anti-inflammatory drugs (NSAIDs) such as Diclofenac are widely used, their long-term administration is associated with significant adverse effects. This has led to a growing demand for safer, plant-based alternatives with comparable efficacy. *Marrubium vulgare* L. (white horehound), a medicinal plant native to the Mediterranean region, is traditionally recognized for its therapeutic benefits and is particularly rich in flavonoids with potential anti-inflammatory properties.

This study employed comprehensive and integrated computational approaches combining Density Functional Theory (DFT) calculations, Molecular Docking, Molecular Dynamics simulations, and Toxicity prediction to evaluate fourteen flavonoids based compounds that were selected from recent phytochemical analysis of *Marrubium vulgare* L. against the COX-1 and COX-2 isoforms, key enzymes in the inflammatory cascade. The results revealed four compounds, Luteolin, Cynaroside (Luteolin-7-O-glucoside), Quercetin, and Rhoifolin (Apigenin-7-O-neohesperidoside), with strong binding affinities and favorable interaction profiles. Among them, Rhoifolin demonstrated the highest binding affinities (− 10.6 kcal/mol for COX-1 and − 10.1 kcal/mol for COX-2), significantly outperforming diclofenac, while also exhibiting excellent predicted biocompatibility and low toxicity risk. Molecular Dynamics simulations further confirmed the stability of its interactions within the active sites.

These findings highlight the therapeutic potential of *Marrubium vulgare* L., flavonoids, particularly Rhoifolin, as effective and safer alternatives to conventional NSAIDs.

Introduction

Inflammation is a complex and highly regulated biological process that represents a crucial defense mechanism of the human body against various internal and external stimuli. This physiological response aims to eliminate harmful agents, repair damaged tissues, and restore homeostasis through the coordinated action of immune cells, such as macrophages and lymphocytes, and a broad range of pro-inflammatory and anti-inflammatory mediators, including cytokines. Despite its beneficial role in the short term, persistent or excessive inflammation can become deleterious, contributing to the pathogenesis of numerous chronic disorders, including rheumatoid arthritis, cardiovascular diseases, neurodegenerative conditions, metabolic syndromes, and certain types of cancer [1–3]

Non-steroidal anti-inflammatory drugs (NSAIDs) remain the mainstay pharmacological agents for managing inflammatory conditions and pain. Diclofenac, a widely prescribed NSAID derived from phenylacetic acid, is recognized for its significant analgesic and anti-inflammatory activities and is used to treat a variety of acute and chronic inflammatory diseases, especially those of rheumatic origin [4–6]. Diclofenac exerts its effects primarily by inhibiting the cyclooxygenase (COX) enzymes, COX-1 and COX-2, which are responsible for the conversion of arachidonic acid to pro-inflammatory prostaglandins and thromboxanes [7, 8]. While COX-1 plays an essential physiological role in maintaining gastric mucosal integrity, renal blood flow, and platelet aggregation, COX-2 is an inducible isoform predominantly expressed during inflammation and is considered a key target for selective anti-inflammatory therapy [9]. However, despite its therapeutic efficacy, long-term administration of diclofenac and other NSAIDs is frequently associated with serious adverse effects, such as gastrointestinal ulcerations, cardiovascular complications, renal toxicity, and, in some cases, hepatotoxicity [6, 10].

This increasing awareness of NSAID-induced side effects has prompted considerable scientific interest in the search for safer, naturally derived alternatives capable of modulating inflammatory pathways with fewer adverse reactions. Over centuries, medicinal plants have served as invaluable sources of bioactive compounds with therapeutic potential against various human diseases [3, 11]. Among these natural products, flavonoids have emerged as a prominent class of

polyphenolic secondary metabolites extensively distributed in fruits, vegetables, herbs, and certain beverages [12, 13]. These molecules exhibit diverse pharmacological activities, including antioxidant, antimicrobial, antiviral, anticancer, cardioprotective, neuroprotective, antidiabetic, hepatoprotective, and notably, anti-inflammatory properties [14–18]. The anti-inflammatory potential of flavonoids is attributed mainly to their ability to modulate key enzymes and signaling pathways involved in inflammation, such as inhibiting COX and lipoxygenase (LOX) enzymes, down regulating pro-inflammatory cytokines, and suppressing oxidative stress [2, 14, 18]

Marrubium vulgare L., commonly known as white horehound, belongs to the Lamiaceae family and has been historically valued in traditional medicine for its diverse therapeutic benefits. It is native to warm areas, notably in including Europe, North Africa, and Central Asia [19]. It has been used to relieve cough, digestive disturbances, skin conditions, rheumatism, and various inflammatory disorders. Recent phytochemical and pharmacological studies have confirmed that the plant contains a rich spectrum of bioactive constituents, such as essential oils, diterpenoids, phenolic acids, coumarins, and notably flavonoids [15, 19–21]. These compounds are believed to contribute significantly to the plant's observed biological activities, which range from anti-inflammatory and antioxidant [14] to antimicrobial, antidiabetic, hepatoprotective, and even anticancer effects [22]. Fourteen flavonoids based compounds were selected from a recent phytochemical analysis [19], are presented in Fig. 1,

Despite this promising profile, no comprehensive in silico investigation has yet systematically evaluated the potential of Marrubium-derived flavonoids as selective COX-2 inhibitors. Given their structural features conducive to modulating inflammation, an in-depth theoretical assessment is warranted to better understand their mechanisms of action at the molecular level. Computational tools such as Density Functional Theory (DFT), molecular docking, Toxicity prediction, and molecular dynamics (MD) simulations play a vital role in modern drug discovery by providing detailed insights into electronic reactivity, binding modes, pharmacokinetic profiles, and dynamic stability [23] .

This study therefore applies an integrated in silico strategy to investigate selected flavonoids from Marrubium vulgare. DFT calculations will elucidate their electronic properties and reactivity, while molecular docking will predict their binding affinity to COX-1 and COX-2 isoenzymes, using diclofenac as a reference NSAID. Toxicity predictions will help assess their pharmacokinetic behavior and safety profile, and MD simulations will evaluate the stability of the most promising flavonoid–COX complexes under physiological conditions.

By combining these complementary approaches, this work aims to identify potential natural COX inhibitors and provide a scientific framework for the rational design of safer, plant-based anti-inflammatory agents.

Materials and Methods

2.1 DFT Computational detail

The compounds analyzed in this study were selected based on the phytochemical analysis reported by Emam et al. (2024) [19]. Their three-dimensional (3D) structures were retrieved from the PubChem database (https://pubchem.ncbi.nlm.nih.gov) and then subjected to computational optimization to ensure a stable geometric configuration [24]. The structures of the studied flavonoids, along with that of Diclofenac (used as a reference drug), are illustrated in Fig. 1. Geometric optimization was performed using Gaussian 16 software [25], using the DFT/B3LYP method with the 6–31G (d,p) basis set [26].

In order to elucidate molecular reactivity, various quantitative descriptors were calculated, such as electronegativity (χ), chemical hardness (η), softness (S), electrophilicity (ω), ionization potential (IP), and electron affinity (A).

$$\eta = \frac{(\mathrm{I}-\mathrm{A})}{2},\ \mu = \frac{-(\mathrm{I}+\mathrm{A})}{2},\ \chi = \frac{(\mathrm{I}+\mathrm{A})}{2},\ \mathrm{S} = \frac{1}{2\eta},\ \omega = \frac{\mu^{2}}{2\eta}$$

These parameters provide essential information on the chemical behavior of the molecules. Reactivity indices were deduced from the energies of the highest occupied (HOMO) and lowest unoccupied (LUMO) molecular orbitals.

2.2 Toxicity prediction

The ProTox platform, which computes hepatoxicity, immunotoxicity, cytotoxicity, aromatase, LD_{50} values, and predicted toxicity class, was used to assess the toxicity of the chosen natural chemicals and reference ligand [27] .

2.3 Molecular Docking Study

After geometry optimization, Gasteiger partial charges were assigned [28], and nonpolar hydrogen atoms were removed using AutoDockTools v1.5.7. All rotatable bonds were defined to allow full ligand flexibility during docking.

The crystal structures of murine cyclooxygenase-1 (COX-1, PDB ID: 3N8Y) [29] and cyclooxygenase-2 (COX-2, PDB ID: 1PXX) [30], both co-crystallized with Diclofenac, were downloaded from the Protein Data Bank (https://www.rcsb.org). Protein structures were prepared using Discovery Studio Visualizer 2021 by removing the co-crystallized ligand, water molecules, and all heteroatoms unrelated to the active site. Polar hydrogen atoms were added and Kollman charges were assigned using AutoDockTools v1.5.7.

Docking simulations were performed using AutoDock Vina v1.1.2 [31] with an exhaustiveness parameter of 8. Binding affinities were expressed as predicted Gibbs free energies (kcal/mol). The resulting docked poses were visualized and analyzed for key interactions, including hydrogen bonds, hydrophobic contacts, and electrostatic interactions, using Discovery Studio Visualizer 2021.

To validate the docking protocol, Diclofenac was removed from the COX-1 and COX-2 crystal structures and re-docked into the respective active sites. The reliability of the docking setup was confirmed by calculating the root-mean-square deviation (RMSD) between the experimental crystallographic pose and the predicted pose.

2.4 Molecular Dynamics

The ligands topology parameters were generated using ACPYPE v. 2023.10.27 with the General Amber force field (GAFF). Prior to molecular dynamics (MD) simulation, the structures of the proteins were first repaired by PDBFixer, a tool designed to fix common structural issues in proteins such as missing atoms, non-standard residues and building missing loops. PDBFixer is part of the OpenMM suite of tools [32]. After that, the topology parameters of the proteins were generated using Amber99sb force field by GROMACS 2024.2 [33]. Each protein-ligand complex was solvated in a cubic box with the Simple Point Charge (SPC) water model and neutralized by adding counter Na + ions. Energy minimization was performed using steepest descent algorithm for up to 50,000 steps with a convergence criterion of Fmax below 200 kJ/mol. The systems were then equilibrated using NVT (canonical) ensemble at 300 K for 500 ps, where the temperature was controlled by V-rescale thermostat, followed by equilibration using NPT (isothermal-isobaric) ensemble for another 500 ps where the temperature and pressure were maintained constant using V-rescale thermostat and Parrinello-Rahman barostat, respectively. Finally, the MD simulations were performed for 100 ns under NPT ensemble. Post-simulation trajectory analysis was conducted using GROMACS tools such as rms, rmsf, gyrate, sasa and h-bond.

Results and discussion

3.1 Geometry optimization

The geometry optimization of compounds was carried out in the vacuum using DFT method at B3LYP/6–31G (d, p) level. The analysis of frontier orbitals, namely the highest-energy occupied molecular orbital (HOMO) and the lowest-energy vacant molecular orbital (LUMO), provides essential information on the electronic reactivity of compounds. The HOMO is associated with a compound's ability to donate electrons, while the LUMO reflects its propensity to accept them. The

energy difference between these two orbitals, HOMO–LUMO gap, is a fundamental indicator of chemical stability and reactivity. A narrow gap suggests high chemical reactivity, due to facilitated electron transfer between orbitals, while a wide gap is generally associated with greater stability and lower reactivity. Thus, the assessment of the HOMO–LUMO gap allows us to anticipate the chemical behavior of compounds, including their reactivity.

3.2 Global chemical reactivity descriptors

The quantum chemical reactivity descriptors computed using density functional theory (DFT) offer a comprehensive understanding of the electronic behavior, stability, and potential reactivity of selected flavonoids alongside the reference compound diclofenac. Ionization potential (I) and electron affinity (A) serve as key indicators of electron-donating and electron-accepting tendencie. The energies of the frontier orbitals and the values of the various reactivity parameters are shown in Table 1.

Table 1
Global chemical reactivity descriptor values for the studied compounds in eV

Compound	I	A	Gap	μ	X		S	ω
Apigenin	5,89535	1,73636	4,15899	-3,81585	3,81585	2,07950	0,48089	3,50103
Apigenin 7-xyloside	5,89236	1,73772	4,15464	-3,81504	3,81504	2,07732	0,48139	3,50320
Apigenin-7-O-diglucuronide -O-hexoside	5,61153	1,14587	4,46566	-3,37870	3,37870	2,23283	0,44786	2,55631
Catechin	5,51439	-0,16925	5,68365	-2,67257	2,67257	2,84182	0,35189	1,25670
Chryseriol	5,86460	1,73092	4,13368	-3,79776	3,79776	2,06684	0,48383	3,48913
Chrysin	6,00120	1,89092	4,11028	-3,94606	3,94606	2,05514	0,48658	3,78840
Luteolin	5,83739	1,71568	4,12171	-3,77653	3,77653	2,06086	0,48524	3,46026
Luteolin 7-lactate	5,90052	1,86017	4,04035	-3,88035	3,88035	2,02017	0,49501	3,72668
Cynaroside	5,88474	1,74752	4,13722	-3,81613	3,81613	2,06861	0,48342	3,51995
Naringenin	5,91739	1,03621	4,88118	-3,47680	3,47680	2,44059	0,40974	2,47648
Quercetin	5,63031	1,68493	3,94538	-3,65762	3,65762	1,97269	0,50692	3,39085
Rhoifolin	6,10814	1,94425	4,16389	-4,02620	4,02620	2,08194	0,48032	3,89306
Vicenin-2	6,21019	2,03188	4,17831	-4,12103	4,12103	2,08916	0,47866	4,06454
Vitexin	5,92038	1,74561	4,17477	-3,83300	3,83300	2,08739	0,47907	3,51920
Diclofenac	5,55194	0,60300	4,94894	-3,07747	3,07747	2,47447	0,40413	1,91371

Among the flavonoids, Apigenin and its derivatives display relatively high ionization potentials (I ≈ 5.89–5.90 eV), indicative of substantial molecular stability. Their electron affinities (A ≈ 1.73 eV) and moderate hardness values (≈ 2.07–2.08 eV) suggest resistance to electronic perturbation and a controlled reactive profile. These observations are consistent with their negative chemical potentials (μ), pointing toward electron-donating behavior, while their moderate electrophilicity indices (ω ≈ 3.5) suggest a balanced potential to act as electrophilic agents [34–36].

Luteolin derivatives exhibit similar behavior with ionization potentials ranging from 5.83 to 5.90 eV and marginally higher softness values compared to apigenin derivatives, which could suggest slightly greater reactivity. Chrysin and chryseriol conform to this trend, with chrysin in particular exhibiting a slightly elevated ionization potential (6.00 eV), indicating

enhanced stability. Quercetin and naringenin distinguish themselves by presenting slightly lower hardness and higher softness values, traits associated with increased molecular reactivity, yet they maintain reasonable electrophilicity indices (ω ≈ 3.39 and 2.47, respectively) [37, 38].

Vicenin-2 and rhoifolin emerge as particularly noteworthy due to their highest ionization potentials (6.21 and 6.10 eV) and electrophilicity indices (ω = 4.06 and 3.89), along with elevated electronegativity and hardness values. These parameters highlight their strong electrophilic character and reduced capacity for electron donation, traits likely to enhance interactions with electron-rich biological environments. The most negative chemical potentials observed for vicenin-2 (− 4.121 eV) and rhoifolin (− 4.026 eV) further support their high electrophilicity. These flavonoids also rank highest in electronegativity (χ > 3.7 eV), which may correlate with their biological efficacy due to favorable interactions with electron-rich biomolecular targets [39] .

Catechin presents an anomaly with a negative electron affinity (A = − 0.17 eV), the lowest electrophilicity (ω = 1.25), and the largest HOMO–LUMO energy gap (5.68 eV), all of which indicate a pronounced resistance to electron uptake and minimal electrophilic activity. This unique profile suggests a dominant nucleophilic character, potentially aligning with antioxidant properties. Catechin also shows the lowest softness (S = 0.35 eV^{-1}), reinforcing its chemical inertness compared to the rest of the flavonoid set [38, 40] .

Diclofenac, used as a reference drug, demonstrates intermediate values for hardness (= 2.47 eV), softness (S = 0.40 eV^{-1}), and electrophilicity index (ω = 1.91 eV), consistent with a balanced chemical profile. Its electronic configuration suggests a trade-off between stability and reactivity that may underpin its recognized anti-inflammatory activity. Notably, apigenin-7-O-diglucuronide-O-hexoside and diclofenac exhibit higher energy gaps (4.47 and 4.95 eV, respectively), which could account for their lower reactivity compared to more inert compounds like Catechin [35, 36, 40] .

Overall, the combined computational analysis underscores distinct electronic features among structurally similar flavonoids. Compounds such as vicenin-2, rhoifolin, and chrysin exhibit electronic configurations conducive to electrophilic interactions and enhanced biological activity, making them promising candidates for further pharmacological exploration. These findings also emphasize the importance of subtle electronic variations in dictating molecular reactivity, target interaction potential, and ultimately, pharmacokinetic behavior, providing a theoretical framework for future drug development efforts involving natural flavonoids.

Taken together, these computational insights not only differentiate the electronic and reactive profiles of the studied flavonoids but also highlight their potential pharmacological relevance in the context of anti-inflammatory activity. Specifically, Vicenin-2, Rhoifolin, and Chrysin demonstrate quantum chemical features that align strongly with favorable anti-inflammatory properties. Their high ionization potentials and electrophilicity indices, coupled with elevated electronegativity and negative chemical potentials, suggest a pronounced ability to engage in electrophilic interactions with electron-rich biological targets, such as enzyme active sites and receptor residues involved in inflammation [35, 39]. These electronic traits may facilitate stronger binding affinities and more effective modulation of inflammatory signaling pathways.

Compared to Diclofenac, the reference compound, these flavonoids display superior or comparable values in key descriptors like electrophilicity and chemical potential, indicating the potential for enhanced or complementary therapeutic effects [40]. In contrast, Catechin, with its low electrophilicity, negative electron affinity, and high HOMO–LUMO gap, appears more chemically inert and better suited for antioxidant roles rather than direct anti-inflammatory intervention [38, 40].

Thus, Vicenin-2, Rhoifolin, and Chrysin emerge as promising natural candidates for further investigation as anti-inflammatory agents. Their electronic configurations not only support stability and reactivity but also suggest the

capacity for biologically relevant interactions. These findings provide a strong theoretical foundation for prioritizing these flavonoids in future drug design and pharmacological screening studies targeting inflammation.

3.3 Toxicity prediction

The toxicity profiles of fourteen flavonoid compounds derived from Marrubium vulgare were predicted using the ProTox-III tool, with Diclofenac as the reference drug. The analysis focused on several types of toxicity, including hepatotoxicity, immunotoxicity, cytotoxicity, neurotoxicity, potential aromatase inhibitory activity, and acute oral toxicity expressed by LD_{50} values and toxicity class.

Overall, the flavonoid compounds showed a favorable safety profile as presented in Table 2, with the majority showing no predicted toxicity in the various categories evaluated. This indicates a wide margin of safety and supports their potential for therapeutic use. However, Apigenin-7-O-diglucuronide-O-hexoside showed potential hepatotoxicity, immunotoxicity, and neurotoxicity. Rhoifolin was identified as potentially immunotoxic. Quercetin, although not toxic in any specific category, has a relatively low LD_{50} value (159 mg/kg), placing it in toxicity class 3, suggesting higher acute toxicity compared to other flavonoids.

With regard to aromatase activity, four compounds (Apigenin, Apigenin-7-O-diglucuronide-O-hexoside, Chryserol, and Chrysin) were predicted to be active, implying possible interactions with estrogen biosynthesis. This effect may be either beneficial or undesirable, depending on the application, and requires further evaluation.

With the exception of quercetin, the LD_{50} values of the flavonoids studied ranged from 832 to 10,000 mg/kg, corresponding to toxicity classes 4 to 6, generally indicating low to moderate acute toxicity. In contrast, the reference drug Diclofenac showed predicted hepatotoxicity and neurotoxicity, with a low LD_{50} (53 mg/kg), placing it in toxicity class 3. This confirms its well-known adverse effect profile and highlights the potential of flavonoids as safer alternatives.

Table 2
Toxicity prediction of White horehound flavonoid compounds and the reference ligands

Compound	Hepatotoxicity	Immunotoxicity	Cytotoxicity	neurotoxicity	Aromatase	LD_{50} (mg/kg)	Class
Apigenin	Inactive	Inactive	Inactive	Inactive	Active	2500	5
Apigenin 7-xyloside	Inactive	Inactive	Inactive	Inactive	Inactive	5000	5
Apigenin-7-O-diglucuronide-O-hexoside	Active	Active	Inactive	Active	Active	1190	4
Catechin	Inactive	Inactive	Inactive	Inactive	Inactive	10000	6
Chryseriol	Inactive	Inactive	Inactive	Inactive	Active	4000	5
Chrysin	Inactive	Inactive	Inactive	Inactive	Active	3919	5
Luteolin	Inactive	Inactive	Inactive	Inactive	Inactive	3919	5
Luteolin 7-lactate	Inactive	Inactive	Inactive	Inactive	Inactive	4000	5
Cynaroside	Inactive	Inactive	Inactive	Inactive	Inactive	5000	5
Naringenin	Inactive	Inactive	Inactive	Inactive	Inactive	5000	5
Quercetin	Inactive	Inactive	Inactive	Inactive	Inactive	159	3
Rhoifolin	Inactive	Active	Inactive	Inactive	Inactive	5000	5
Vicenin-2	Inactive	Inactive	Inactive	Inactive	Inactive	832	4
Vitexin	Inactive	Inactive	Inactive	Inactive	Inactive	832	4
Diclofenac	Active	Inactive	Inactive	Active	Inactive	53	3

3.4. Molecular Docking Study

3.4.1. Validation of Docking Protocol

Validation of the molecular docking protocol is a critical step to ensure the reliability and predictive power of the simulations. In this study, the accuracy of the docking setup was verified by re-docking Diclofenac (Fig. 2) into the active sites of COX-1 (PDB code 3N8Y) and COX-2 (PDB code 1PXX). The RMSD values were found as 0.325 Å for COX-1 and 1.286 Å for COX-2, both well below the commonly accepted threshold of 2.0 Å for small-molecule re-docking. These results confirm the robustness of the docking protocol and the reliability of the predicted ligand-enzyme interactions for the tested Marrubium vulgare flavonoids.

3.4.2. Binding Energy to COX Isoforms

Molecular docking simulations were performed to investigate the inhibitory potential of flavonoid compounds isolated from white horehound against the cyclooxygenase isozymes COX-1 and COX-2, which are central to the inflammatory cascade. Compounds were ranked according to their binding affinity values (kcal/mol), where more negative values indicate stronger predicted binding. The observed binding affinities for the tested flavonoids ranged from − 8.4 to − 10.6 kcal/mol, suggesting favorable interactions with both isoforms. These values suggest that the flavonoids may act as competitive inhibitors by occupying the NSAID-binding site of cyclooxygenase isozymes, mimicking the binding mode of

traditional inhibitors such as Diclofenac [41]. The results of docking analysis scores of all tested docked ligands are summarized in Table 3.

Among the 14 compounds screened, Rhoifolin demonstrates the highest binding affinity to COX-1 (− 10.6 kcal/mol) and COX-2 (− 10.1 kcal/mol), suggesting a strong interaction and potential inhibitory effect on both isoforms. This is notably more favorable than the reference drug Diclofenac, which shows lower binding affinities of − 8.5 kcal/mol and − 8.6 kcal/mol toward COX-1 and COX-2, respectively.

Other compounds such as Cynaroside (-9.3 / -9.7 kcal/mol), Luteolin (-9.5 / -8.9 kcal/mol), and Quercetin (-9.1 / -9.4 kcal/mol) also demonstrate relatively high binding energies, indicating potential dual inhibitory activity with a preference for one isoform over the other in some cases. Compounds like Vicenin-2, while still active, exhibited comparatively lower affinities. These differences in binding energy values highlight the structural influence of glycosylation and hydroxyl substitutions on the binding strength and selectivity toward the two COX isoforms. Glycosylated flavonoids such as Rhoifolin and Cynaroside were consistently more potent, suggesting that the sugar moiety increases the number of polar contacts within the active site and improves the ligand's orientation and stabilization.

Table 3
Binding affinity of White horehound flavonoid compounds to COX-1 and COX-2

		Affinity (kcal/mol)	
	Compound	**COX-1**	**COX-2**
1	Apigenin	-9.0	-8.9
2	Apigenin 7-xyloside	-9.3	-8.8
3	Apigenin-7-O-diglucuronide -O-hexoside	-9.2	-8.6
4	Catechin	-9.2	-9.0
5	Chryseriol	-9.1	-8.7
6	Chrysin	-8.7	-9.1
7	Luteolin	-9.5	-8.9
8	Luteolin 7-lactate	-9.0	-9.0
9	Cynaroside (Luteolin 7-O-glucoside)	-9.3	-9.7
10	Naringenin	-8.9	-8.8
11	Quercetin	-9.1	-9.4
12	Rhoifolin (Apigenin-7-O-neohesperidoside)	-10.6	-10.1
13	Vicenin-2	-8.5	-8.4
14	Vitexin	-9.1	-8.9
	Diclofenac	-8.5	-8.6

3.4.3. Ligands interactions with COX-1 Enzyme

Both COX-1 and COX-2 isoforms share a high degree of structural and functional similarity, with approximately 67% sequence identity [42]. Despite this homology, structural differences within the active site - particularly the presence of a secondary binding pocket in COX-2 - provide a critical basis for selective inhibition. This side pocket, absent in COX-1,

results from the substitution of isoleucine at position 523 in COX-1 with the smaller valine residue in COX-2, thereby creating additional space within the NSAID-binding site. This conformational change led to unlocking this secondary binding pocket and unveiling the polar amino acid ARG513 which is considered the ameliorating COX-2 selectivity [43] .

Molecular docking studies have indicated that COX-1 may act as an intracellular target for flavonoids, such as those isolated by [44]. These compounds are able to form hydrogen bonds with key residues, specifically arginine and/or tyrosine, located in the gate of the active site and to sterically inhibit the conversion of arachidonic acid (AA) to prostaglandin H2 (PGH2) by preventing its entry into the active site [44, 45].

The detailed molecular interaction analysis presented in Table 4 and Fig. 3 further supports the docking scores. Rhoifolin, the top binder, forms multiple strong hydrogen bonds with key residues such as HIS90, GLN192, GLN350, in the COX-1 active site. It also establishes hydrophobic and electrostatic contacts, particularly with HIS95 and PRO514, which may enhance its binding stability within the active site pocket.

Luteolin, with a high binding affinity of -9.5 kcal/mol, interacts through hydrogen bonds with key residues such as HIS90, GLN192, and is further stabilized by hydrophobic interactions with PRO514. Cynaroside (Luteolin 7-O-glucoside) forms 10 hydrogen bonds with COX-1 active site residues such as GLN192, GLU347, TYR355, and ASN515, along with hydrophobic and electrostatic interactions involving HIS581. However, despite this interaction network, its binding affinity was found to be lower than that of the aglycone Luteolin. This suggests that glycosylation at the 7-OH position may impair optimal accommodation within the COX-1 active site, possibly due to steric hindrance or reduced complementarity with key residues. The sugar moiety may limit deep penetration into the hydrophobic channel or interfere with key interactions required for stronger binding, thereby diminishing its inhibitory potential compared to the non-glycosylated form.

In contrast, Diclofenac, although clinically effective, exhibits a relatively limited interaction profile. It forms only one hydrogen bond, specifically with TYR385, and relies primarily on hydrophobic interactions involving residues such as VAL349 and ALA527. This reduced network of polar interactions contributes to its lower binding affinity compared to more interactive ligands.

Notably, TYR385 is a key catalytic residue involved in the radical-mediated oxygenation of arachidonic acid, and its interaction is considered critical for the inhibitory action of many NSAIDs. However, Diclofenac’s inability to engage with additional polar or charged residues- such as those accessible in the COX-2-specific secondary pocket- limits its selectivity and may account for some of its adverse effects associated with COX-1 inhibition.

3.4.4. Ligands interactions with COX-2 Enzyme

COX-2, though highly homologous to COX-1, possesses a more spacious active site and a distinctive side pocket, allowing selective inhibitors to bind more deeply.

Rhoifolin exhibited a strong and selective binding profile toward COX-2, characterized by multiple stabilizing interactions, including hydrogen bonds with ALA199, PHE210, and HIS386, as well as electrostatic contacts with HIS207. Particularly, its interaction with TRP387, a residue essential for selective COX-2 inhibition, reinforces its potential as a dual or COX-2-preferential inhibitor. Our findings are consistent with previous studies, which reported an affinity value of -10,5 kcal/mol for the same compound toward COX-2. Notably, those studies also identified three amino acid residues (HIS207, HIS388 and PHE210) involved in the binding site that are identical to those observed in our analysis, further supporting the reliability of our results and suggesting a conserved interaction pattern [46].

These computational results align with in vitro evidence, where Rhoifolin demonstrated anti-inflammatory and neuroprotective effects by enhancing neuronal viability, reducing apoptosis and oxidative stress, and suppressing pro-inflammatory cytokines in an epilepsy model. These effects were mechanistically linked to inhibition of the NF-

κB/iNOS/COX-2 axis [47]. This convergence between in silico predictions and experimental outcomes strongly supports the role of Rhoifolin as a promising COX-2-targeting anti-inflammatory and neuroprotective agent.

Similarly, Cynaroside and Quercetin established interactions with HIS386, HIS388, and TRP387, residues crucial for NSAID binding. The hydrogen bond network and π–π stacking with aromatic residues enhance their stabilization in the COX-2 pocket.

In contrast, Diclofenac formed only a single hydrogen bond (TYR385) and interacted mainly with hydrophobic residues such as VAL349 and TRP387, in line with its non-selective profile [48] .

Table 4
Molecular interaction of the ligands with COX-1 and COX-2

Isoforms	Compounds	Binding affinity (kcal/mol)	Hydrogen bonds	Electrostatic bonds	Hydrophobic bonds
COX-1	Rhoifolin	-10.6	HIS90 (2.58 Å), GLN192 (2.87 Å, 2.07), GLN350 (2.02, 2.27, 2.50 Å), PRO191 (1.83 Å)	HIS95	HIS95, and PRO514
	Luteolin	-9.5	HIS90 (2.32 Å), GLN192 (2.00 Å, 2.34), PRO514 (2.50 Å)	-	PRO514
	Cynaroside	-9.3	GLN192 (2.96 Å, 2.75 Å), ASN 515 (2.50 Å, 2.31 Å), GLU 347 (1.97 Å), TYR 355 (1.95 Å), PRO514 (2.87 Å), GLN351 (3.72 Å), GLY354 (2.92 Å), SER353 (3.69 Å)	HIS581	HIS581
	Diclofenac	-8.5	TYR385 (2.18 Å)	-	VAL349, ALA527, ILE523, LEU352
COX-2	Rhoifolin	-10.1	ALA199 (2.03 Å), PHE210 (2.26 Å, 2.60 Å), THR212 (1.89 Å), HIS386 (3.07 Å, 2.70 Å), TRP387 (3.24 Å)	HIS207	HIS207, HIS388, ALA202
	Cynaroside	-9.7	ALA199 (2.06 Å, 2.26 Å), ASN382 (2.42 Å, 2.82 Å), HIS388 (2.96 Å)	HIS207	HIS386, HIS207, HIS388
	Quercetin	-9.2	HIS386 (2.72 Å), HIS388 (3.03 Å, 3.74 Å), TRP387 (2.20 Å)	HIS207	HIS386, HIS207, HIS388,
	Diclofenac	-8.6	TYR385 (2.76 Å)		TRP387, VAL349, VAL523, ALA527, LEU352

3.5 Molecular Dynamic Results

Root Mean Square Deviation (RMSD) was used to assess the structural stability and convergence of the complexes over time by quantifying the average distance between backbone atoms relative to initial structures. (Fig. 5A) illustrates the RMSD profiles for Cox-1 protein in complex with different ligands (Diclofenac, Luteolin, Luteolin-7-O-glucoside (Cynaroside) and Rhoifolin). Notably, Rhoifolin exhibited the highest RMSD values with an average of 0.25 ± 0.04 nm, which indicates higher structural fluctuations in Cox-1 induced by this ligand. On the other hand, Luteolin showed the lowest and more stable RMSD values (average 0.19 ± 0.02 nm) compared to the reference compound Diclofenac (average 0.21 ± 0.02 nm) and the other studied ligands.

In Cox-2 Protein (Fig. 5B), Luteolin-7-O-glucoside showed the highest RMSD values (average 0.20 ± 0.03 nm) compared to the reference compound Diclofenac (average 0.18 ± 0.02 nm) and the other ligands. The RMSD values for Quercetin were

relatively stable till 80 ns then started to increase until the end of the simulation time. In contrast, Rhoilfolin showed the most stable RMSD values (average 0.17 ± 0.01 nm) among the other ligands.

The Root Mean Square Fluctuation (RMSF) analysis of Cox-1 and Cox-2 proteins in complex with various ligands is illustrated in (Fig. 6). This analysis provides insights into residual fluctuations and flexibility by quantifying the average deviation of each residue's backbone atoms from their time-averaged positions. In Cox-1 protein (Fig. 6A), Luteolin-7-O-glucoside notably increased the residual fluctuations in many regions like 70–82, 213–216 and 293–295, while Luteolin increased fluctuations in residue 514. All the three tested compounds reduced fluctuations and stabilized the region 553–561.

For Cox-2 protein (Fig. 6B), the tested compounds increased residual fluctuations in different regions for example, Quercetin increased RMSF in regions 105–111 and 368–370, Luteolin-7-O-glucoside increased RMSF in regions 213–215, 369–370 and 555–565, while Rhoifolin increased RMSF in regions 515–517 and 526–559.

The Radius of Gyration (RG) analysis reveals insights into the overall compactness and structural stability of the complexes. For Cox-1 protein (Fig. 7A), all the ligands showed RG values with an average of 2.43 nm. Luteolin and Rhoifolin exhibited almost the same RG values as the reference compound Diclofenac during the whole simulation time, while Luteolin-7-O-glucoside started to show lower RG values from 55 ns till the end of the simulation time suggesting a more compact protein structure.

For Cox-2 protein (Fig. 7B), all the ligands showed nearly the average RG of 2.44 nm. Quercetin induced higher RG values starting from 85 ns till the end of the simulation compared to the other ligands.

The analysis of Solvent-Accessible Surface Area (SASA) offers information about the exposure of the protein surface to surrounding solvent molecules during molecular dynamics simulations. In case of Cox-1 protein (Fig. 8A), Luteolin and Rhoifolin showed almost the same SASA values as the reference compound, while Luteolin-7-O-glucoside exhibited lower SASA values from 55 ns till the end of the simulation compared to the other ligands.

For Cox-2 protein (Fig. 8B), a similar trend emerges where Luteolin-7-O-glucoside and Rhoifolin showed almost the same SASA values as the reference compound, while Quercetin exhibited higher SASA values from 60 ns till the end of the simulation compared to the other ligands.

From hydrogen bonding analysis with Cox-1 protein, the reference compound Diclofenac and Luteolin exhibited lower number of hydrogen bonds (1–3) suggesting weaker interactions with the protein (Fig. 9A & B). On the other hand, Luteolin-7-O-glucoside and Rhoifolin formed higher numbers of hydrogen bonds with a max of 6 and 8 bonds, respectively (Fig. 9C & D).

In case of Cox-2 protein, the reference compound Diclofenac also showed the lowest number of hydrogen bonds (max 2) while many periods showed no bond formation (Fig. 10A). Quercetin, Luteolin-7-O-glucoside and Rhoifolin showed higher number of hydrogen bonds, up to 6 bonds, suggesting stronger interactions with Cox-2 protein (Fig. 10B, C & D).

Molecular dynamics simulations revealed significant differences in the interactions between ligands and COX-1 and COX-2 proteins stability, comparable to that of Diclofenac, but Rhoifolin caused the worst structural variations with COX-1. While Rhoifolin maintained a steady structure, Luteolin-7-O-glugoside showed the largest RMSD deviations for COX-2. Ligand specific residual flexibilities with unique effects on protein regions were identified by RMSF analysis.

Measurements of compactness (RG) and solvent exposure (SASA) verified structural differences, such as greater compaction for Cox-1 under the influence of luteolin-7-O-glucoside and increased exposure to quercetin for Cox-2. Lastly, compared to diclofenac, there were more hydrogen bonds with luteolin-7-O-glucoside and rhoifolin, indicating stronger

interactions. These findings open the door for further research on the binding affinities and functional characteristics of these ligands, highlighting their potential as viable candidates for therapeutic applications targeting Cox proteins.

Conclusion

This study evaluated the anti-inflammatory potential of fourteen flavonoid compounds derived from Marrubium vulgare L. in order to identify natural alternatives to conventional non-steroidal anti-inflammatory drugs (NSAIDs). A combination of Density Functional Theory (DFT), molecular docking, molecular dynamics simulations and structural analysis revealed that several of the compounds exhibited promising activity.

DFT calculations highlighted Vicenin-2, Rhoifolin, and Chrysin as stable and reactive molecules, providing a theoretical basis for their potential biological activity. Molecular docking studies further revealed that Rhoifolin, Cynaroside, Luteolin and quercetin exhibit strong potential as natural cyclooxygenase (COX) inhibitors. Among them, Rhoifolin emerged as a particularly promising dual inhibitor, demonstrating superior binding affinity and interaction profiles compared to Diclofenac, support further in vitro and in vivo evaluation for anti-inflammatory activity.

Molecular dynamics simulations revealed significant variations in ligand-protein stability. Rhoifolin induced the greatest structural deviation in COX-1, while Cynaroside showed the highest RMSD for COX-2. RMSF analysis indicated the presence of distinct residue flexibility patterns that were influenced by specific ligands. Further confirmation of the observed differences was provided by structural metrics, including radius of gyration (Rg) and solvent-accessible surface area (SASA). Notably, COX-1 compaction was observed under Cynaroside, while increased solvent exposure of COX-2 was seen under Quercetin. Hydrogen bonding analyses demonstrated that both Cynaroside and Rhoifolin formed more hydrogen bonds than diclofenac, indicating stronger and more stable interactions. Importantly, the toxicity profile of ibuprofen (LD_{50} = 53 mg/kg, class 3) was found to be more concerning than that of most of the tested compounds, underscoring the value of pursuing safer, plant-derived alternatives.

In conclusion, the flavonoids identified in Marrubium vulgare L. exhibit a favourable safety profile, suggesting their potential as candidates for further in silico modelling and experimental validation in the development of natural anti-inflammatory agents with reduced toxicity compared to conventional drugs. Rhoifolin, cynaroside and luteolin in particular emerge as promising compounds for subsequent pharmacological investigation and therapeutic development.

Declarations

Conflict of interest

The authors declare that they have no competing interests. All authors approved the final manuscript.

Author Contribution

Fatima KADRI: Conceptualization; Investigation; Methodology; Data curation; Formal analysis; Bibliographic research; Writing original draft ; Writing-review and editing.Sofiane Benmetir :Molecular dynamics simulation and results analysisMohammed Arab AIT TAYEB: Conceptualization; Investigation; Methodology; Data curation; Formal analysis; Bibliographic research; Writing original draft ; Writing-review and editing.Khadidja SMAIL: Conceptualization; Investigation; Methodology; Data curation; Formal analysis; Bibliographic research; Writing original draft ; Writing-review and editing.Fatima zohra Fadel:Toxicity assessment, calculations, and interpretation.Karim Ouadah :Literature review, manuscript proofreading, and overall manuscript revisionNoureddine Tchouar :Review, proofreading, and overall manuscript revision.Jésus Vicente de Julián-Ortiz : Review, manuscript proofreading, and overall manuscript revision

Acknowledgement

Acknowledge:'J. V. de J.-O. acknowledges for the financial support provided by theUniversitat de València's special actions program, reference ComPPETEUV-INV-AE-3677056.'

Data Availability

All the data generated in the work are presented in the manuscript.

References

1. Medzhitov, R., *Origin and physiological roles of inflammation*. Nature, 2008. 454(7203): p. 428–435.
2. Chagas, M.d.S.S., et al., *Flavonols and Flavones as Potential anti-Inflammatory, Antioxidant, and Antibacterial Compounds*. Oxidative Medicine and Cellular Longevity, 2022. 2022(1): p. 9966750.
3. Lin, Z., et al., *Anti-Inflammatory Activity of Mulberry Leaf Flavonoids In Vitro and In Vivo.* 2022. 23(14): p. 7694.
4. Krum, H., et al., *Blood Pressure and Cardiovascular Outcomes in Patients Taking Nonsteroidal Antiinflammatory Drugs*. Cardiovascular Therapeutics, 2012. 30(6): p. 342–350.
5. Vascular *and upper gastrointestinal effects of non-steroidal anti-inflammatory drugs: meta-analyses of individual participant data from randomised trials*. The Lancet, 2013. 382(9894): p. 769–779.
6. Ventura-Martínez, R., et al., *Quercetin decreases the antinociceptive effect of diclofenac in an arthritic gout-pain model in rats*. Journal of Pharmacy and Pharmacology, 2021. 73(10): p. 1310–1318.
7. Smith, W.L., D.L. DeWitt, and R.M. Garavito, *Cyclooxygenases: structural, cellular, and molecular biology*. Annu Rev Biochem, 2000. 69: p. 145–82.
8. Hassan, R.A., et al., *Naringin and Hesperidin Counteract Diclofenac-Induced Hepatotoxicity in Male Wistar Rats via Their Antioxidant, Anti-Inflammatory, and Antiapoptotic Activities.* Oxid Med Cell Longev, 2021. 2021: p. 9990091.
9. Warner, T.D., et al., *Nonsteroid drug selectivities for cyclo-oxygenase-1 rather than cyclo-oxygenase-2 are associated with human gastrointestinal toxicity: A full in vitro analysis.* Proceedings of the National Academy of Sciences, 1999. 96(13): p. 7563–7568.
10. Rao, P. and E.E. Knaus, *Evolution of nonsteroidal anti-inflammatory drugs (NSAIDs): cyclooxygenase (COX) inhibition and beyond*. J Pharm Pharm Sci, 2008. 11(2): p. 81s-110s.
11. Cragg, G.M. and D.J. Newman, *Natural products: a continuing source of novel drug leads*. Biochim Biophys Acta, 2013. 1830(6): p. 3670–95.
12. Kumar, S. and A.K. Pandey, *Chemistry and biological activities of flavonoids: an overview.* ScientificWorldJournal, 2013. 2013: p. 162750.
13. Al-Khayri, J.M., et al., *Flavonoids as Potential Anti-Inflammatory Molecules: A Review.* 2022. 27(9): p. 2901.
14. Ghedadba, N., et al., *Evaluation of in vitro antioxidant and in vivo anti-inflammatory potentialof white Horehound (Marrubium vulgare) Leaves*. International Journal of Pharmaceutical Sciences Review and Research, 2016. 41(1): p. 252–259.
15. Namoune, I., et al., *Antioxidant and Anti-inflammatory Activities of Organic and Aqueous Extracts of Northeast Algerian Marrubium vulgare*. Phytothérapie, 2018. 16.
16. Al-Ishaq, R.K., et al., *Flavonoids and Their Anti-Diabetic Effects: Cellular Mechanisms and Effects to Improve Blood Sugar Levels*. Biomolecules, 2019. 9(9).
17. Maleki, S.J., J.F. Crespo, and B. Cabanillas, *Anti-inflammatory effects of flavonoids*. Food Chem, 2019. 299: p. 125124.

18. Shamsudin, N.F., et al., *Flavonoids as Antidiabetic and Anti-Inflammatory Agents: A Review on Structural Activity Relationship-Based Studies and Meta-Analysis*. Int J Mol Sci, 2022. 23(20).
19. Emam, M., et al., *Anti-Alzheimer's Potency of Rich Phenylethanoid Glycosides Extract from Marrubium vulgare L.: In Vitro and In Silico Studies*. 2024. 17(10): p. 1282.
20. Aćimović, M., et al., *Marrubium vulgare L.: A Phytochemical and Pharmacological Overview*. Molecules, 2020. 25(12).
21. Amri, B., et al., *Marrubium vulgare L. Leave Extract: Phytochemical Composition, Antioxidant and Wound Healing Properties.* 2017. 22(11): p. 1851.
22. Lodhi, S., et al., *Marrubium vulgare L.: A review on phytochemical and pharmacological aspects.* 2017. 6(4): p. 429–452.
23. Lionta, E., et al., *Structure-based virtual screening for drug discovery: principles, applications and recent advances*. Curr Top Med Chem, 2014. 14(16): p. 1923–38.
24. Kim, S., et al., *PubChem Substance and Compound databases*. Nucleic Acids Res, 2016. 44(D1): p. D1202-13.
25. Frisch, M.e., et al., *Gaussian 16*. 2016, Gaussian, Inc. Wallingford, CT.
26. Becke, A.D., *Density-functional thermochemistry. I. The effect of the exchange-only gradient correction*. The Journal of Chemical Physics, 1992. 96(3): p. 2155–2160.
27. Banerjee, P., et al., *ProTox-II: a webserver for the prediction of toxicity of chemicals*. Nucleic Acids Res, 2018. 46(W1): p. W257-w263.
28. Gasteiger, J. and M.J.T.L. Marsili, *A new model for calculating atomic charges in molecules.* 1978. 19: p. 3181–3184.
29. Sidhu, R.S., et al., *Comparison of cyclooxygenase-1 crystal structures: cross-talk between monomers comprising cyclooxygenase-1 homodimers*. Biochemistry, 2010. 49(33): p. 7069–79.
30. Rowlinson, S.W., et al., *A novel mechanism of cyclooxygenase-2 inhibition involving interactions with Ser-530 and Tyr-385.* J Biol Chem, 2003. 278(46): p. 45763–9.
31. Trott, O. and A.J. Olson, *AutoDock Vina: Improving the speed and accuracy of docking with a new scoring function, efficient optimization, and multithreading*. Journal of Computational Chemistry, 2010. 31(2): p. 455–461.
32. Eastman, P., et al., *OpenMM 7: Rapid development of high performance algorithms for molecular dynamics*. PLOS Computational Biology, 2017. 13(7): p. e1005659.
33. Abraham, M.J., et al., *GROMACS: High performance molecular simulations through multi-level parallelism from laptops to supercomputers*. SoftwareX, 2015. 1–2: p. 19–25.
34. Chattaraj, P.K., U. Sarkar, and D.R. Roy, *Electrophilicity Index.* Chemical Reviews, 2006. 106(6): p. 2065–2091.
35. Parr, R.G., L.v. Szentpály, and S. Liu, *Electrophilicity Index*. Journal of the American Chemical Society, 1999. 121(9): p. 1922–1924.
36. Parr, R.G. and Y. Weitao, *Density-Functional Theory of Atoms and Molecules*. 1994: Oxford University Press.
37. Li, Y., et al., *Quercetin, Inflammation and Immunity.* 2016. 8(3): p. 167.
38. Middleton, E., Jr., C. Kandaswami, and T.C. Theoharides, *The Effects of Plant Flavonoids on Mammalian Cells:Implications for Inflammation, Heart Disease, and Cancer*. Pharmacological Reviews, 2000. 52(4): p. 673–751.
39. Hussein, R. and A. El-Anssary, *Plants Secondary Metabolites: The Key Drivers of the Pharmacological Actions of Medicinal Plants*, in *Herbal Medicine*, P. Builders, Editor. 2018, IntechOpen: Rijeka.
40. Cherkasov, A., et al., *QSAR Modeling: Where Have You Been? Where Are You Going To?* Journal of Medicinal Chemistry, 2014. 57(12): p. 4977–5010.
41. Warner, T.D. and J.A. Mitchell, *Cyclooxygenases: new forms, new inhibitors, and lessons from the clinic*. Faseb j, 2004. 18(7): p. 790–804.

42. Hawash, M., et al., *Molecular docking studies and biological evaluation of isoxazole-carboxamide derivatives as COX inhibitors and antimicrobial agents*. 3 Biotech, 2022. 12(12): p. 342.
43. Kurumbail, R.G., et al., *Structural basis for selective inhibition of cyclooxygenase-2 by anti-inflammatory agents*. Nature, 1996. 384(6610): p. 644–8.
44. Wu, C.-M., et al., *Antiplatelet Effect and Selective Binding to Cyclooxygenase (COX) by Molecular Docking Analysis of Flavonoids and Lignans*. 2007. 8(8): p. 830–841.
45. Warner, T.D., S. Nylander, and C. Whatling, *Anti-platelet therapy: cyclo-oxygenase inhibition and the use of aspirin with particular regard to dual anti-platelet therapy*. Br J Clin Pharmacol, 2011. 72(4): p. 619–33.
46. Rahmouni, F., et al., *Antioxidant and antiproliferative effects of Teucrium polium extract: computational and in vivo study in rats*. Toxicol Mech Methods, 2024. 34(5): p. 495–506.
47. Qi, H., et al., *Rhoifolin attenuates damage to hippocampal neuronal culture model of acquired epilepsy in vitro by regulating NF-κB/iNOS/COX-2 axis*. 2022. 14(3): p. 116–123.
48. Ahmadi, M., et al., *Non-steroidal anti-inflammatory drugs: recent advances in the use of synthetic COX-2 inhibitors*. RSC Medicinal Chemistry, 2022. 13(5): p. 471–496.

Figures

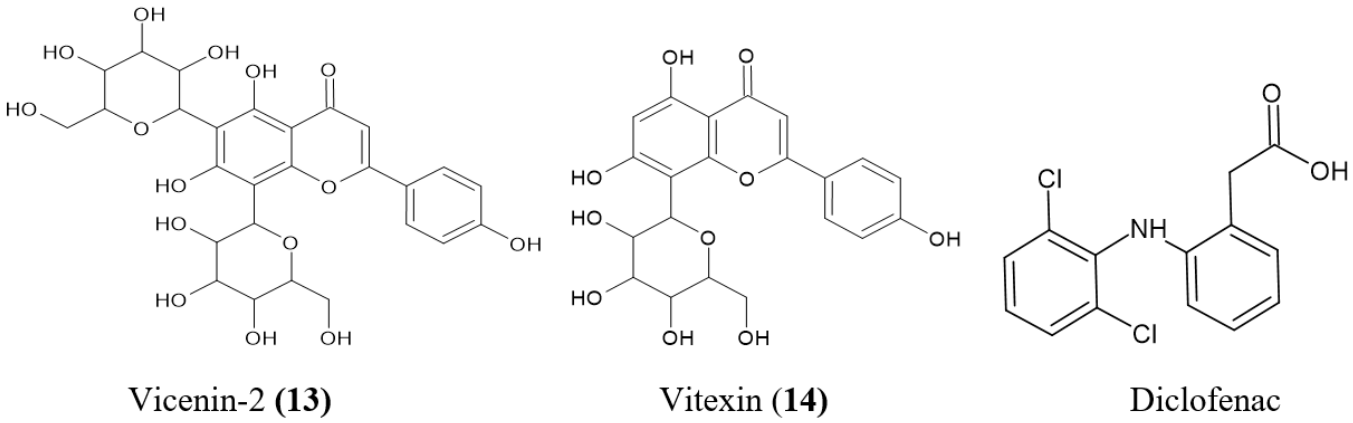

Figure 1

Structures of selected flavonoids contained in the *Marribium vulgare* L. plant and the structure of Diclofenac

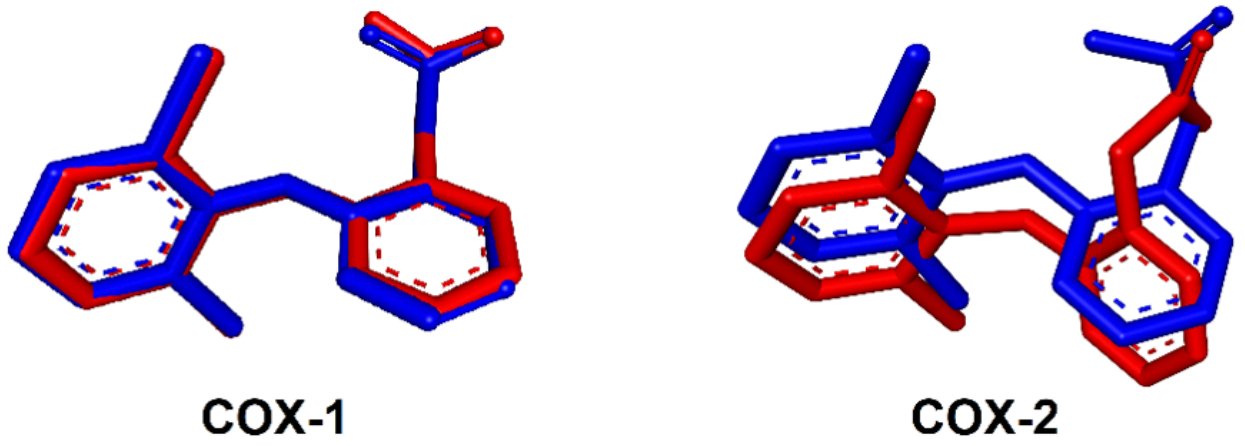

Figure 2

Superimposition of the co-crystallized ligand (blue) and the re-docked pose (red) in the active site of COX-1 and COX-2.

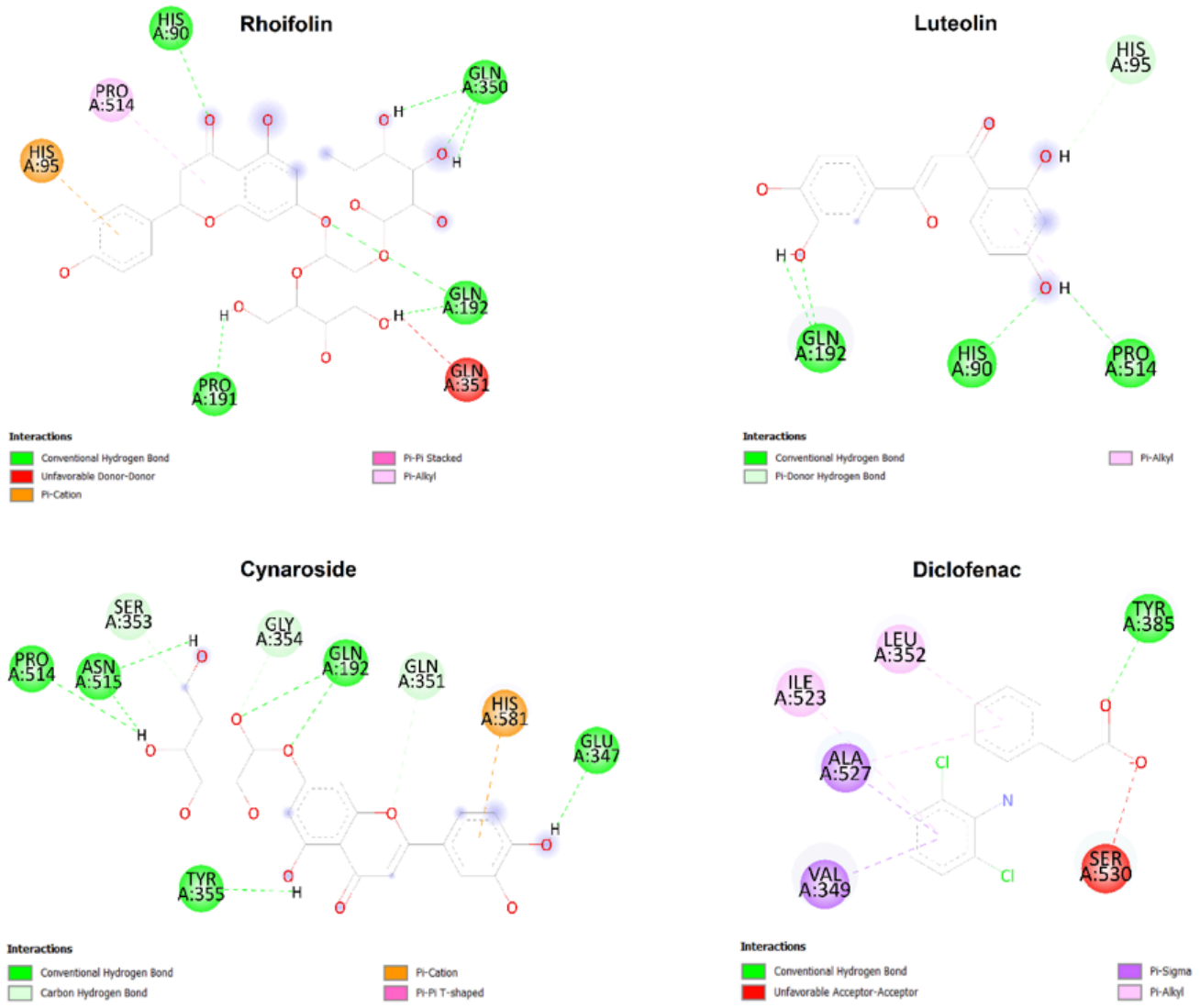

Figure 3

2D interaction of Rhoifolin, Luteolin, Cynaroside and Diclofenac with COX-1 enzyme.

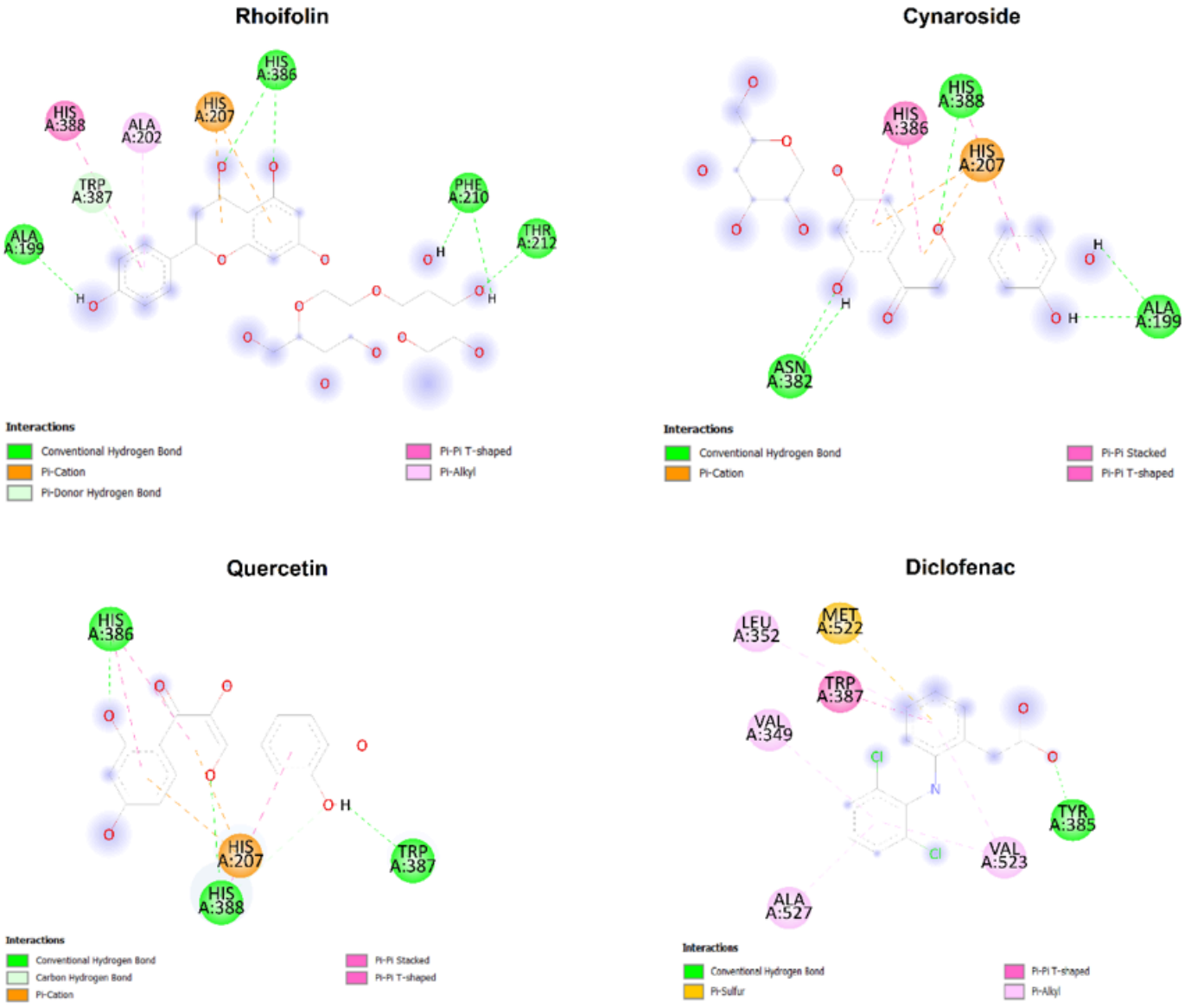

Figure 4

2D interaction of Rhoifolin, Cynaroside, Quercetin and Diclofenac with COX-2 enzyme.

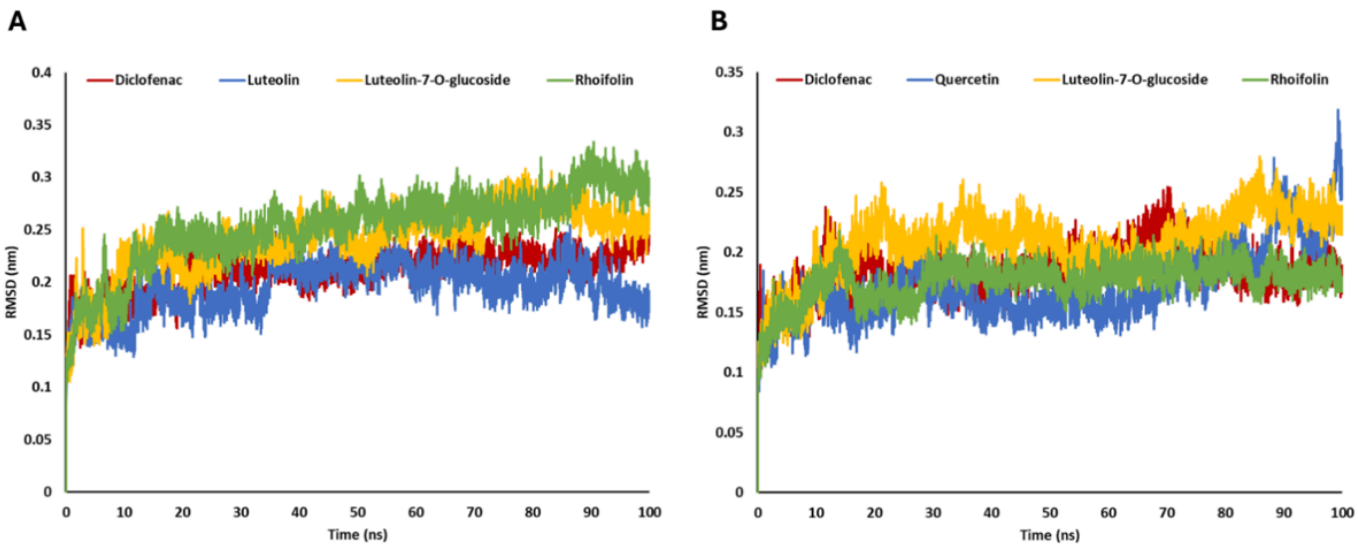

Figure 5

RMSD of Cox-1 (A) and Cox-2 (B) proteins in complex with different ligands over 100 ns MD simulations.

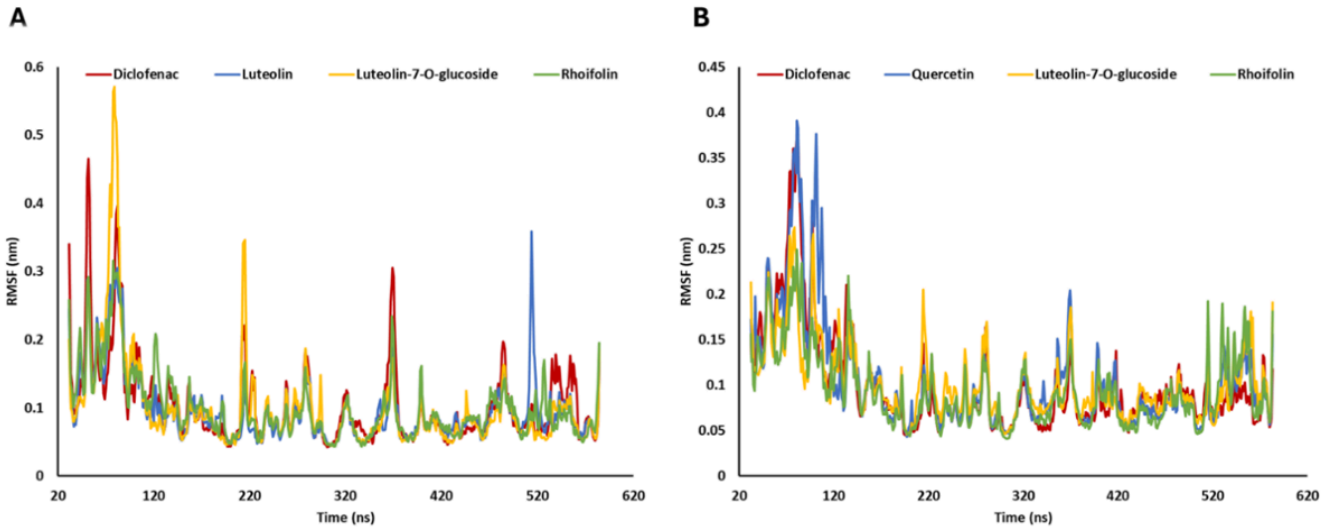

Figure 6

RMSF of Cox-1 (A) and Cox-2 (B) proteins in complex with different ligands over 100 ns MD simulations.

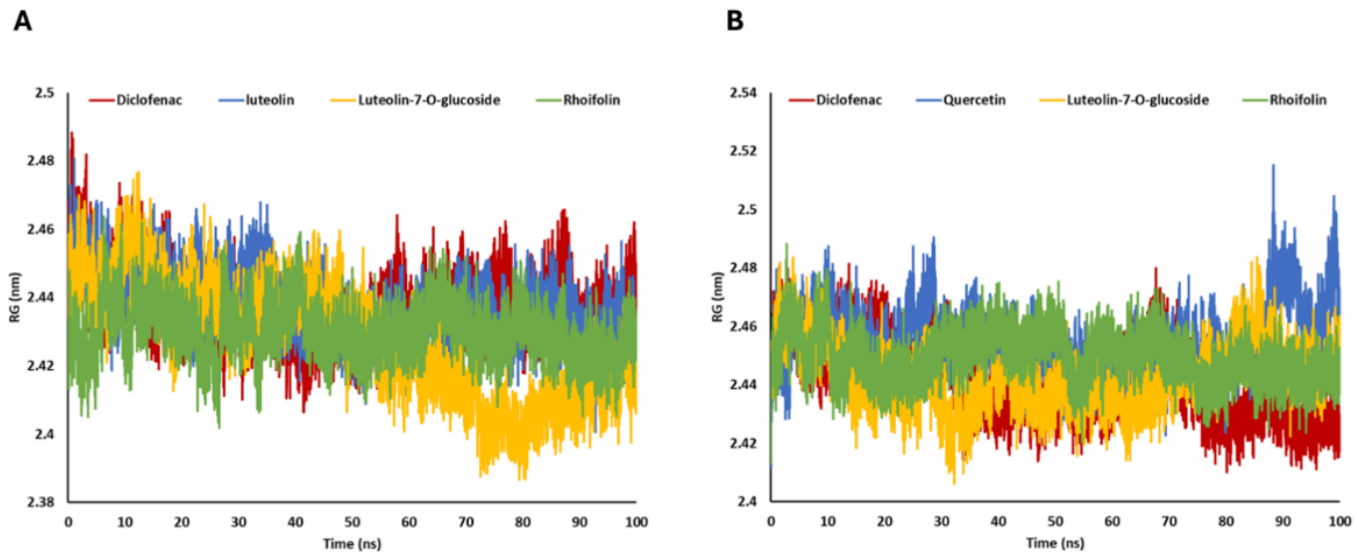

Figure 7

RG of Cox-1 (A) and Cox-2 (B) proteins in complex with different ligands over 100 ns MD simulations.

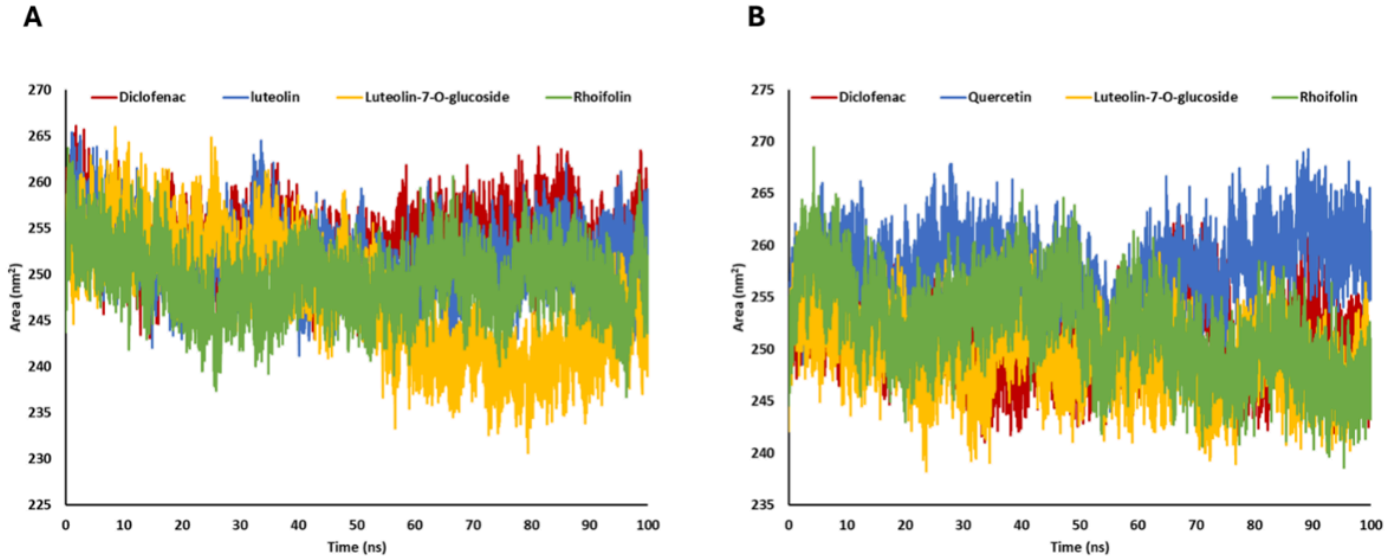

Figure 8

SASA of Cox-1 (A) and Cox-2 (B) proteins in complex with different ligands over 100 ns MD simulations.

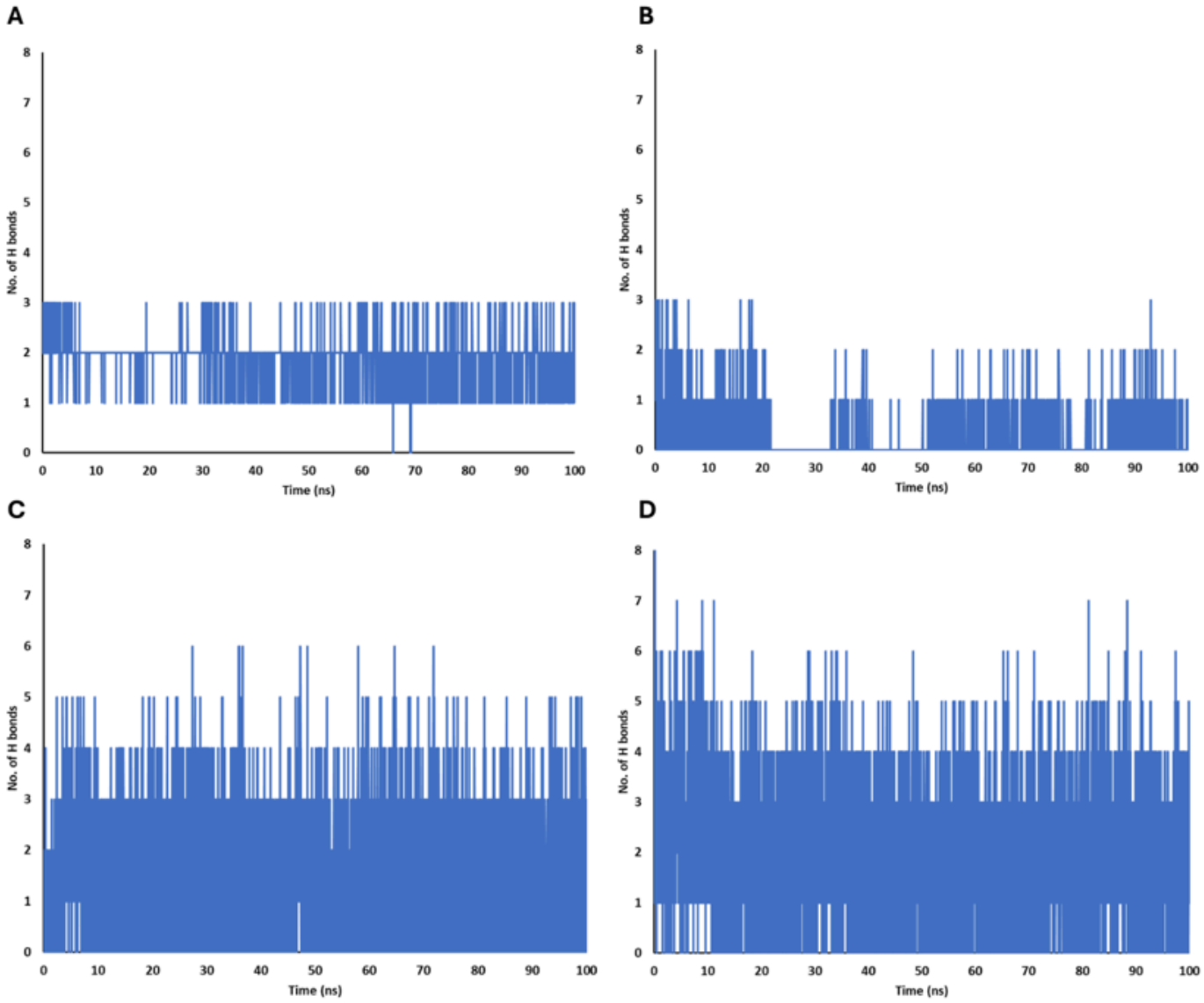

Figure 9

Number of hydrogen bonds formed between Cox-1 protein and Diclofenac (A), Luteolin(B), Luteolin-7-O-glucoside (C), and Rhoifolin (D) over 100 ns MD simulations.

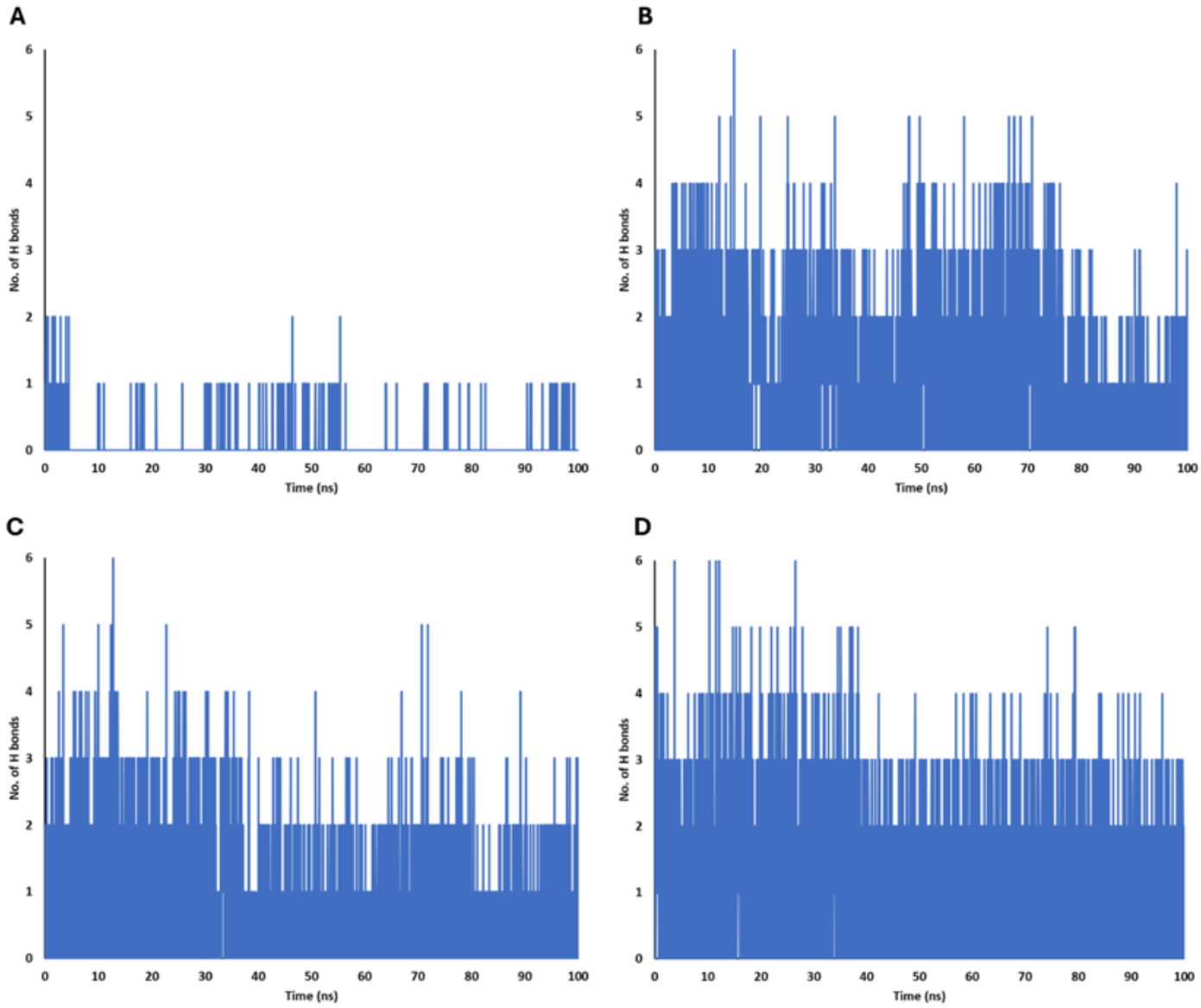

Figure 10

Number of hydrogen bonds formed between Cox-2 protein and Diclofenac (A), Quercetin (B), Luteolin-7-O-glucoside (C), and Rhoifolin(D) over 100 ns MD simulationsj.softx.2015